A Description of Water Masses in Nootka Sound and Estimation of Diffusivity (κ) and Upward Velocity (w) in Muchalat Inlet Using Temperature, Salinity, and Dissolved Oxygen

Oceanography Senior Thesis
Ocean 445

Julie Ann Koehlinger

May 31, 2015

University of Washington, School of Oceanography
Box 357940, Seattle, Washington 98195
jkoehl@uw.edu

Acknowledgements

I would like to thank Charlie Eriksen for all of his time and guidance throughout this project. Catherine Young and Robert Daniels for their assistance with UCTD data analysis. Many thanks to Jemima Rama and the rest of the students who participated in the cruise for their assistance in collecting CTD and UCTD data. Last but certainly not least, I thank the crew of the Thomas G. Thompson and the University of Washington School of Oceanography, for making it all possible.

Abstract

Nootka Sound is a rarely studied fjord estuary on the west coast of Vancouver Island, Canada. Using CTD and UCTD casts, water property data was collected from the entrance sill, main basin, and through the three inlets in the sound. Temperature, salinity, and dissolved oxygen data were used to identify water masses. Temperature and salinity data collected from two different transects through Muchalat Inlet allowed the calculation of diffusivity (κ) and vertical velocities (w) in this inlet. Our results show evidence for temperature advection, with estimated κ ranging from 2.8×10^{-5} to 4.5×10^{-5} m^2s^{-1} and a localized downwelling event, with estimated w of -5.4×10^{-6} m^2s^{-1} to -2.0×10^{-5}.

Introduction

Nootka Sound is a fjord estuary located on the west side of Vancouver Island, Canada. It is comprised of a main entrance basin and three inlets, Muchalat, Tlupana, and Tahsis. Its main river inputs are the Gold River (which empties into Muchalat Inlet), and the Tahsis and Tsowwin rivers (which empty into Tahsis Inlet). Smaller rivers, the Sucwoa and Conuma, drain into Tlupana inlet.

The typical pattern of estuarine circulation is that saline water enters at depth from the ocean, upwells and mixes with freshwater supplied by river discharge, and exits near the surface (Geyer and Cannon, 1982). Circulation is one of the drivers of dissolved oxygen levels below the photic zone, where primary production and therefore production of oxygen, is occurring. Since oxygen below the surface layer is consumed during the biological process of respiration, deep water renewal is required to maintain life below the surface layer. Without deep water renewal, decreasing oxygen levels result in hypoxia. These oxygen minimum zones (OMZ) affect the composition and distribution of species in the water column including bacteria and archaea (Zaikova et. al., 2010), zooplankton (Keister and Tuttle, 2013) and fish (Breitburg et. al., 1997).

Nootka Sound, like many fjord estuaries, is bounded by an entrance sill. Sills impact the physical processes of the estuary. They restrict new water masses from entering the estuary to occasions when upwelling is strong enough to bring water up and over the sill, or when conditions favor formation of intermediate level water masses that can also travel over the sill. This cold, saline water then sinks to renew the deep water of the estuary (Pickard, 1963, Anderson and Devol, 1973, Masson, 2002). Nootka Sound is expected to follow this circulation pattern.

In addition to the entrance sill of Nootka Sound, secondary sills (Tahsis Narrows and Williamson Sill) are located in Tahsis and Muchalat Inlets. Since two upwelling events would be required for deep water to enter these inlets, flow is likely further restricted at these secondary sills. As a consequence, the deep water beyond these sills may be entirely different water masses.

Stratification of the water column also impacts circulation and mixing. Nookta Sound is a highly stratified estuary. This means that there is a relatively shallow mixed layer and the remainder of the water column is stably stratified. This stable stratification inhibits futher mixing in the deeper parts of the inlets.

Nootka Sound is not well studied, with most oceanographic measurements being taken in Muchalat Inlet (Tully, 1937, Pickard, 1963). Pickard (1963) did survey Tahsis and Tlupana Inlets. Tully's data was collected in July and his investigation of circulation focused on tidal mixing. Pickard collected data in May, June, and July and discussed relationships between sill depth of the estuaries he studied to the temperature and salinity characteristics of the various inlets. Published data from Nootka Sound has not been updated since Pickard's 1963 study.

The only available wintertime data is a daily measurement of sea surface temperature (SST) and salinity at the Nootka Point Lighthouse (49° 13.8' N 126° 19.8' W) taken by the British Columbia Shore Station Oceanographic Program. This data has been collected daily at high tides occurring between 0600 and 1800 since 1934. Also available is a monthly average of SST and salinity (http://www.dfo-mpo.gc.ca).

This study will characterize and describe Nootka Sound's water masses using temperature, salinity, and dissolved oxygen measurements from the ship's CTD sensor. Comparisons will be made between water column properties of the main basin as well as each inlet in order to identify discrete water masses. Additionally, the Underway CTD's

measurements will be used in comparison with the stationary ship CTD to examine temperature and salinity changes in Muchalat Inlet over the course of the research cruise. These changes will allow the calculation of a diffusivity value (κ) and an upward velocity (w), which also will assist in assessing mixing of the waters of the estuary in a time when water mass exchange is not actively occurring.

Methods

We collected data aboard the research vessel *Thomas G Thompson* from 11-21 December, 2014. We performed stationary conductivity, temperature, and depth (CTD) casts at thirty-six stations (Fig. 1 and Table 1) in Nootka Sound using a Seabird SBE 911plus rosette CTD and collected water samples using Niskin sampling bottles.

Name of Station	Latitude	Longitude	Date/Time (UTC)	Depth of Cast (m)	Significant Features
N02	49° 31.01’ N	126° 43.19’ W	12 Dec 23:33	47	Entrance Sill
N03b	49° 34.88’ N	126° 36’ W	13 Dec 01:33	87	
N04	49° 35.83’ N	126° 32.10’ W	13 Dec 02:40	137	
N05	49° 37.77’ N	126° 29.85’ W	13 Dec 03:37	161	
N06	49° 40.68’ N	126° 29.51’ W	16 Dec 09:53	110	
N07	49° 41.03’ N	126° 34.93’ W	20 Dec 05:39	140	Mouth of Tahsis Inlet
N08	49° 37.98’ N	126° 36.52’ W	20 Dec 10:49	150	
M01	49° 37.77’ N	126° 03.95’ W	14 Dec 18:34	130	Head of Muchalat Inlet
M02	49° 39.40’ N	126° 05.59’ W	14 Dec 19:58	177	
M03	49° 40.00’ N	126° 06.30’ W	15 Dec 11:03	313	
M04	49° 40.22’ N	126° 08.07’ W	14 Dec 15:41	345	
M06	49° 40.02’ N	126° 10.33’ W	14 Dec 13:09	359	
M07	49° 39.72’ N	126° 12.48’ W	14 Dec 12:04	351	
M08	49° 39.27’ N	126° 14.00’ W	14 Dec 07:20	361	
M09	49° 38.80’ N	126° 16.10’ W	14 Dec 06:14	325	
M10	49° 38.59’ N	126° 18.42’ W	14 Dec 04:05	279	
M11	49° 38.49’ N	126° 20.95’ W	14 Dec 01:59	279	
M13	49° 39.31’ N	126° 23.03’ W	13 Dec 23:42	75	Williamson Sill
M14	49° 39.36’ N	126° 24.97’ W	13 Dec 22:43	143	
M15	49° 38.98’ N	126° 27.00’ W	13 Dec 05:03	185	Mouth of Muchalat Inlet

M16	49° 38.60’ N	126° 25.82’ W	13 Dec 18:53	113	
M17	49° 38.16’ N	126° 22.69’ W	13 Dec 20:04	129	
T01	49° 54.89’ N	126° 39.46’ W	18 Dec 07:25	60	Head of Tahsis Inlet
T02	49° 54.47’ N	126° 39.56’ W	17 Dec 15:07	90	
T03	49° 53.99’ N	126° 39.41’ W	17 Dec 13:53	160	
T04	49° 52.97’ N	126° 39.52’ W	17 Dec 12:55	190	
T05	49° 51.91’ N	126° 39.58’ W	18 Dec 04:53	189	
T06	49° 50.98’ N	126° 39.7’ W	17 Dec 10:23	185	
T07	49° 49.73’ N	126° 39.58’ W	17 Dec 09:34	160	
T08	49° 48.03’ N	126° 39.11’ W	17 Dec 05:46	124	
T23	49° 45.53’ N	126° 38.01’ W	20 Dec 02:30	100	Tsowwin Narrows
T24	49° 45’ N	126° 37.8’ W	20 Dec 03:20	98	Tsowwin Narrows
L01	49° 46.88’ N	126° 28.19’ W	16 Dec 18:53	135	Head of Tlupana Inlet
L02	49° 45.79’ N	126° 25.23’ W	16 Dec 17:42	80	
L03	49° 43.16’ N	126° 28.80’ W	16 Dec 16:04	208	
L04	49° 42.01’ N	126° 30.18’ W	16 Dec 10:45	236	Mouth of Tlupana Inlet

Table 1. Ship CTD Stations with latitude and longitude of each station, date and time of cast, depth of CTD cast measurements, and any significant bathymetric or other features.

The CTD casts provided temperature, salinity, and dissolved oxygen concentration data. Niskin bottle samples provided *in situ* dissolved oxygen concentrations, which were calculated using Winkler titration after the Chesapeake Bay Institute technique (Carpenter, 1965), and were used to verify the CTD oxygen sensor. The Oceanscience Seabird Underway CTD (UCTD) was used on the final day of the cruise to collect an additional transect of temperature and salinity data through Muchalat Inlet (Figure 1 and Table 2).

Due to the positioning of the CTD sensor at the bottom of the rosette, most stationary CTD measurements started at a depth of 5m, and the few measurements that were obtained at depths of less than 5m were not used so that the comparisons made between CTD casts utilized a consistent set of data. For the same consistency of comparison, UCTD cast data of less than 5m was also not utilized.

UCTD Cast Number	Latitude	Longitude	Date/Time (UTC)	Depth of Cast (m)	Nearest ship CTD station
856	49° 39.02’ N	126° 27.4’ W	20 Dec 20:09	164	M04
852	49° 39.48’ N	126° 24.89’ W	20 Dec 19:57	158	M06
851	49° 39.14’ N	126° 22.7’ W	20 Dec 19:46	161	M07
849	49° 38.51’ N	126° 20.66’ W	20 Dec 19:35	156	M08
848	49° 38.63’ N	126° 18.84’ W	20 Dec 19:27	154	M09
846	49° 38.8’ N	126° 16.65’ W	20 Dec 19:16	135	M10
845	49° 39.15’ N	126° 14.18’ W	20 Dec 19:03	145	M11
843	49° 39.74’ N	126° 12.1’ W	20 Dec 18:51	124	M13
842	49° 40’ N	126° 10.36’ W	20 Dec 18:43	84	M14
840	49° 40.23’ N	126° 8.26’ W	20 Dec 18:32	95	M15

Table 2. Underway CTD Stations with latitude and longitude of each station, date and time of cast, depth of UCTD cast measurements, and nearest ship CTD station.

Data collected were plotted for comparison of temperature, salinity, and percent saturation of dissolved oxygen through the Main Basin of Nootka Sound and separately through each inlet. Filled contour plots were made using a Matlab interpolation script (C. Eriksen, pers. comm.). Other scripts by Eriksen were used to interpret UCTD data and seawater properties were calculated with scripts found in the SeaWater Matlab library by Morgan and Pender (2010).

The salinity sensor on both UCTD probes was found to drift over the time of the cruise and required the determination of a correction factor. This was accomplished by adjusting UCTD conductivity by an offset so that deep temperature and salinity curves matched those from ship CTD casts done nearby. Correction factors were determined by Catherine Young (pers. comm.) and applied to the UCTD casts used to determine calculations of upward velocity (w), as detailed in the Discussion section of this paper.

Results

Stationary CTD Measurements

Temperatures in Muchalat Inlet varied between 7.5 and 14°C with the majority of the salinity measurements between 28 and 33 PSU. Maximum oxygen saturation level was 91.2% and the minimum level reached 0% (Figure 2a). Tlupana Inlet had a similar temperature range

(7.5 to 14°C) with slightly higher salinities, the majority being between 29 and 33 PSU. Maximum oxygen saturation levels were also slightly lower at 85.5%. Minimum values remained greater than 4.9% (Figure 2b). Tahsis Inlet had a much narrower temperature range, between 8.5 and 12.5°C. Tahsis was also relatively fresher, with salinity measurements between 27.5 and 32.5 PSU. Oxygen saturations ranged between 5.8 and 89.3% (Figure 2c). The Nootka Entrance sill had a very narrow temperature range (10.7 to 10.9°C) as well as salinity range (29.8 to 31.1 PSU). Oxygen saturation at the sill ranged from 89.8 to 93.2% (Figure 2d).

The temperature contour along Muchalat Inlet shows a wedge of warmer water around the 50 meter level that expands upward through the water column and warms further toward the head of the inlet (Figure 3). Four stations were sampled in Tlupana Inlet. These four stations all showed water warmer than that of the main Nootka Sound basin at depths less than 50 meters (Figure 4).

Tahsis Inlet shows two pockets of relatively warmer water near station N7 and stations T4, T3, T2, and T1. Stations T23 and T24 are the center of cooler water at shallow depths and warmer water at deeper depths. These two stations are found on either side of the Tsowwin River as it empties into Tahsis Inlet. Isohalines shift around stations T23 and 24 as well as near station T7, where Tahsis Narrows enters Tahsis Inlet (Figure 5).

Underway CTD Measurements

UCTD casts in Muchalat Inlet showed a decrease in temperature from the time of the ship CTD casts at the beginning of the cruise to the time of the UCTD casts on the final day of the cruise. Salinity also decreased in this time (Figure 6).

Discussion

TS plots show distinct water masses in each inlet. The coldest, most saline, and least oxygenated end member in Muchalat Inlet is seen in the deepest part of the basin at depths below 125 m. This water mass is below the depths of both the Nootka Entrance Sill (50 m) as well as Williamson Sill (75 m). Its low percent oxygen saturation further indicates that this water has been present in the inlet for some time. The peak in temperature shows another water mass extending through most of the water column at middle salinity ranges. A third water mass, fresher, with higher oxygen content, but cooler in temperature than the second mass, likely entered the inlet most recently.

Tlupana Inlet has a similar structure to Muchalat, with a deep, poorly oxygenated end member, a higher temperature, better oxygenated secondary mass, and a fresher, cooler, well oxygenated third mass.

Tahsis Inlet has two distinct end members. The slightly warmer and better oxygenated water mass is seen at Tsowwin Narrows, where it is influenced by influx from the Tsowwin River. The colder and less oxygenated water mass is found on the other side of the Tsowwin Narrows sill (85 m).

The temperature of the Nootka Entrance Sill station is cooler than the water of similar salinity in every inlet. Its salinity is fresher than the water of similar temperature in every inlet. This indicates that at the time of measurement, the sill water is not the source water for any of the inlets.

A striking feature of each temperature contour plot is the presence of an elevated temperature wedge in the shallow depth of each inlet. This temperature wedge is most pronounced in Muchalat Inlet (Figure 3), where at the head of the inlet, the temperatures in the

wedge ranges from 12.5 – 14°C and occupies the 20-50 m depth range. The temperature wedge gradually tapers toward the mouth of the inlet, mostly disappearing by CTD station M10. Water at the Nootka Entrance Sill station (CTD station N2), which is the source water for entry into the inlet at the time of the research cruise, is only around 10.5°C.

The temperature wedge in Tlupana Inlet (Figure 4) shows a similar temperature range at the head of the inlet and largely disappears at the mouth of the inlet. Although the temperature wedge in Tahsis Inlet (Figure 5) is not as warm, with a maximum temperature around 13°C, it is still present at the head of the inlet and some temperature elevation is seen at the mouth of the inlet near CTD station N7. The Tsowwin River outflow, which empties into Tahsis Inlet at Tsowwin narrows, (between CTD stations T23 and T24) is clearly influencing the present temperature and salinity in the middle region of the inlet.

We can speculate on the origin of the temperature wedge by first examining the physical depth in all inlets. We see that the base of the wedge is at a depth of approximately 50m in each inlet (Figures 3,4,5). The depth of the Nootka Sound Entrance Sill is also approximately 50m. Warmer water entering the Sound over the sill is more likely to remain a shallow water mass, depending on its salinity profile and it is likely that this temperature wedge is a remnant of an earlier mass of water which flowed over the sill.

We next examine the average SST at Nootka Point Lighthouse (Table 3), and here we see that the average temperatures in July, August, and September are 15.3, 15.9, and 15.0 °C, respectively. (Daily temperatures for 2014 are only available until June 30, 2014.)

The CTD cast taken at station N02 shows a variation of less than 0.2°C through the water column of the sill. It is likely that water flowing over the sill and into the inlets is initially well

mixed and has a relatively uniform temperature. Water entering the Sound earlier in the summer appears to have introduced a temperature signature that has persisted into the winter.

	Jan	Feb	Mar	Apr	May	June	July	Aug	Sept	Oct	Nov	Dec
Temperature (°C)	7.2	6.8	7.8	10.1	12.3	13.8	15.3	15.9	15.0	12.2	9.4	7.8
Salinity (PSU)	26.5	25.7	27.5	26.2	27.6	28.4	30.1	31.0	30.9	28.5	23.0	24.7

Table 3. Average monthly SST and Salinity as measured at Nootka Point Lighthouse. (http://www.pac.dfo-mpo.gc.ca)

By examining UCTD casts that were taken on the final day of the cruise, we can also glean information on the eventual fate of the temperature wedge. UCTD stations located in closest proximity to the CTD stations show a small but noticeable drop in temperature when plotted side by side with nearby CTD stations. Figure 7 shows a typical comparison of UCTD and CTD stations (UCTD cast #840 and CTD station M4).

Using the equations for conservation of temperature:

$$\frac{\partial T}{\partial t} + u\frac{\partial T}{\partial x} + v\frac{\partial T}{\partial y} + w\frac{\partial T}{\partial z} = -\frac{\partial}{\partial z}\left(-\kappa\frac{\partial T}{\partial z}\right) \qquad (1)$$

we now examine the role of temperature advection. We assume here that along channel advection ($u\frac{\partial T}{\partial x}$) and cross channel advection ($v\frac{\partial T}{\partial y}$) are small enough to be insignificant, and that $\frac{\partial T}{\partial z}$ is, if not zero, then quite small and we can neglect $w\frac{\partial T}{\partial z}$ and $\frac{\partial \kappa}{\partial z}\frac{\partial T}{\partial z}$ near the temperature maximum. Under these conditions, our conservation equation then simplifies to:

$$\frac{\partial T}{\partial t} = \kappa\,\frac{\partial^2 T}{\partial z^2} \qquad (2)$$

Using the temperature differences between the UCTD and stationary ship CTD stations, we can calculate a diffusivity value, κ (Figure 7 and Table 4) by determining where $\frac{\partial T}{\partial z}$ crosses through zero and $\frac{\partial^2 T}{\partial z^2}$ is robust. Since we have only two time points of data collection, $\frac{\partial T}{\partial t}$ was

estimated by taking the temperature difference between each dataset at corresponding depths and then dividing that difference by the elapsed time between casts. As the maximum temperature of the UCTD cast was deeper than the maximum temperature of the CTD cast, values for κ were calculated for +/- 5m depths where $\frac{\partial T}{\partial z}$ approached zero and changed sign. These values were then averaged to determine the estimated κ value.

Stationary CTD Station	UCTD cast number	Depths Averaged	Estimated $\frac{\partial T}{\partial t}$ (°C s^{-1})	Estimated $\frac{\partial^2 T}{\partial z^2}$ (°C m^{-2})	Estimated κ (m^2 s^{-1})
M4	840	32-41 m	6.9 x 10^{-7}	-1.5 x 10^{-2}	4.5 x 10^{-5}
M9	846	36-45 m	4.1 x 10^{-7}	-1.4 x 10^{-2}	2.8 x 10^{-5}
M11	849	39-48 m	2.6 x 10^{-7}	-1.3 x 10^{-2}	3.5 x 10^{-5}
M15	856	42-51 m	6.1 x 10^{-7}	-1.8 x 10^{-2}	3.3 x 10^{-5}

Table 4. Kappa (κ) values calculated individually over +/- 5m of $\frac{\partial T}{\partial z} \approx 0$, then averaged together to determine estimated κ value.

The equations for conservation of salinity are identical to conservation of temperature (substituting salinity for temperature):

$$\frac{\partial S}{\partial t} + u\frac{\partial S}{\partial x} + v\frac{\partial S}{\partial y} + w\frac{\partial S}{\partial z} = -\frac{\partial}{\partial z}\left(-\kappa\frac{\partial S}{\partial z}\right) \quad (3)$$

Still assuming that along channel and cross channel advections are small enough to be insignificant, we eliminate $u\frac{\partial S}{\partial x}$ and $v\frac{\partial S}{\partial y}$. However, $\frac{\partial S}{\partial z}$ does have relevance because it never reaches zero, and we now have the salinity equation:

$$\frac{\partial S}{\partial t} + w\frac{\partial S}{\partial z} = -\frac{\partial}{\partial z}\left(-\kappa\frac{\partial S}{\partial z}\right) \quad (4)$$

or:

$$w = \left(\kappa\frac{\partial^2 S}{\partial z^2} - \frac{\partial S}{\partial t}\right) / \frac{\partial S}{\partial z} \quad (5)$$

This equation was used along with salinity differences between the UCTD and CTD stations to calculate upward velocity values at several stations (Figure 8 and Table 5). The same

depths used in the calculation of average κ were used to determine $\frac{\partial S}{\partial z}$ and $\frac{\partial^2 S}{\partial z^2}$. Like the estimation of $\frac{\partial T}{\partial t}$, $\frac{\partial S}{\partial t}$ was estimated by taking the salinity difference between each dataset at corresponding depths and then dividing that difference by the elapsed time between casts. The values for w were then individually calculated and averaged to obtain the estimated w value.

Stationary CTD Station	UCTD cast number	Depths Averaged	Estimated $\frac{\partial S}{\partial z}$ (m^{-1})	Estimated $\frac{\partial^2 S}{\partial z^2}$ (m^{-2})	Estimated $\frac{\partial S}{\partial t}$ (s^{-1})	Estimated w ($m\ s^{-1}$)
M4	840	32-41 m	-4.3×10^{-2}	-4.9×10^{-3}	3.4×10^{-7}	-1.4×10^{-5}
M9	846	36-45 m	-3.2×10^{-2}	-3.3×10^{-3}	5.0×10^{-7}	-2.0×10^{-5}
M11	849	39-48 m	-4.6×10^{-2}	-2.6×10^{-3}	3.2×10^{-7}	-1.2×10^{-5}
M15	856	42-51 m	-3.7×10^{-2}	-9.4×10^{-4}	2.3×10^{-7}	-5.4×10^{-6}

Table 5. Upward velocity (w) values calculated individually over +/- 5m of the depths where $\frac{\partial T}{\partial z} \approx 0$, (as determined by calculations of κ), then averaged together to determine the estimated w value.

The UCTD temperature maximum is deeper than the ship CTD temperature maximum, and our upward velocity calculation results in a negative value. (The UCTD salinity values, after applying the appropriate correction factor, are lower throughout the inlet than the earlier measured CTD values.) This tells us that some amount of downwelling or downward wind forced flow has taken place. With a drop in the maximum temperature level of approximately 5 meters in a 6-day period, this implies a w of approximately -10^{-5} m/s. We see similar estimated order of magnitude w values at stations M4, M9, and M11 and a decrease in w as we move toward the mouth of the inlet.

The salinity curve of both CTD and UCTD stations has a more rapid rate of change in the upper portion of the profile than it does at the deeper portion of the profile, resulting in a divergence of the salinity flux. That is, if the salinity in the shallow depths is changing at a faster rate then the deeper water, the net contribution of mixing will serve to reduce the salinity by flattening the curve as it moves toward equilibrium, resulting in the observed freshening of the

20-40 meter depth range.

Estimates of diffusivity in fjords have utilized direct measurements in Puget Sound, with an average κ of 3.6 x 10^{-3} m^2s^{-1} (Mickett et.al., 2004) and as well as calculations from a salinity budget in the Strait of Georgia (Masson, 2002) with an average κ of 1.1 x 10^{-3} m^2s^{-1}. These values are considerably higher than the estimated κ calculated here. The κ value in Nootka Sound is, however, a similar order of magnitude (10^{-5} m^2s^{-1}) as previously calculated values in the open ocean (Banyte et.al., 2012, Ledwell, et. al., 1993.)

In the absence of larger scale physical processes, even a small amount of vertical motion can significantly affect the water column. If our measurement of w is used to determine the amount of time it will take for a parcel of water to move downward in the water column, a 50m depth is reached somewhere between 29 and 52 days (using the highest and lowest estimated w values.) In this time period, we would expect the temperature wedge that we see in Muchalat Inlet to dissipate. Since we have no measurements in the months prior to the research cruise, it is impossible to tell at what temperature water entered the inlet, how long it took to travel horizontally through the inlet, and what role diffusivity and vertical motion played in transporting the temperature wedge through the inlet.

Conclusions

Nootka Sound and its inlets currently show a stagnant deep water layer, as evidenced by it relatively uniform temperature and salinity and very low (in Muchalat Inlet reaching zero) percentage of oxygen saturation. At the time of this study, there appear to be only smaller scale physical process at work in mixing in this fjord, but we do see effects of diffusivity and vertical velocity, with estimated κ ranging from 2.8 x 10^{-5} to 4.5 x 10^{-5} m^2s^{-1} and estimated w of -5.4 x 10^{-6} m^2s^{-1} to -2.0 x 10^{-5}.

In a highly stratified estuary such a Nootka Sound, salinity changes rapidly in the first 5m. Future studies should endeavor to better capture this data, whether through more careful positioning of the stationary CTD sensor or utilization of the UCTD. One limitation of the UCTD is that it does not capture dissolved oxygen data, and this is also useful information in ascertaining whether or not there has been recent renewal of the deep water or whether there is ongoing stagnation. Repeated data measurements over time can determine the most accurate measurement of κ and w values, but this requires considerable investment in ship time or deployment of equipment to frequently collect water column property data.

References

Anderson, J.J., and A.H. Devol. 1973. Deep water renewal in Saanich Inlet, an intermittently anoxic basin. *Estuar. Coastal Mar. Sci.* 1: 1-10.

Banyte, D., T. Tanhua, M. Visbeck, D. W. R. Wallace, J. Karstensen, G. Krahmann, A. Schneider, L. Stramma, and M. Dengler 2012. Diapycnal diffusivity at the upper boundary of the tropical North Atlantic oxygen minimum zone, *J. Geophys. Res*., 117, C09016.

Breitburg, D.L., Loher, T., Pacey, C.A., and Gerstein, A. 1997. Varying effects of low dissolved oxygen on trophic interactions in an estuarine food web. *Ecol. Monogr*. 67: 489–507.

Carpenter, J.H. 1965. The Chesapeake Bay Institute technique for the Winkler dissolved oxygen method. *Limnol and Oceangr*. 10: 141-143. University Press.

Fisheries and Oceans Canada. Nootka Point Lighthouse Daily and Time Averaged datasets. http://www.pac.dfo-mpo.gc.ca/science/oceans/data-donnees/lighthouses-phares/data/nootkaday.txt (daily dataset) and http://www.pac.dfo-mpo.gc.ca/science/oceans/data-donnees/lighthouses-phares/data/nootkaa.txt (averages dataset). Accessed 29 May 2015.

Geyer, W.R. and Cannon G.A. 1982. Sill processes related to deep water renewal in a fjord. *J. Geophys. Res. – Oceans Atmos*. 87: 7985-7996.

Keister, J.E., and Tuttle, L.B. 2013. Effects of bottom-layer hypoxia on spatial distributions and community structure of mesozooplankton in a sub-estuary of Puget Sound, Washington, U.S.A. Limnol. Oceanogr., 58(2): 667–680.

Lafond, C. and Pickard, G. 1975. Deepwater Exchanges in Bute Inlet, British Columbia. *J. Fish. Res. Bd. Can*. 32 2075-2089.

Ledwell, J. R., A. J. Watson, and C. S. Law (1993), Evidence for slow mixing across the pycnocline from an open-ocean tracer-release experiment, *Nature* 364, 701–703.

Masson, D. 2002. Deep Water Renewal in the Strait of Georgia. *Estuar. Coastal and Shelf Sci.* 54: 115–126.

Mickett, J.B., Gregg, M.C., and Seim, H.E. 2004. Direct measurements of dipycnal mixing in a fjord reach – Puget Sound's Main Basin. *Estuar. Coastal Shelf Sci.* 59: 539-558
Morgan, P. and Pender, L. 22 December 2010. SeaWater Matlab Library Release 3.3 http://www.cmar.csiro.au/datacentre/ext_docs/seawater.htm. Accessed 10 January 2015.

Pickard, G. 1963. Oceanographic Characteristics of Inlets of Vancouver Island, British Columbia. *J. Fish. Res. Bd. Can*. 20(5) 1109-1144.

Tully, J. 1937. Oceanography of Nootka Sound, *J. Biol. Bd. Can*. 3(1) 43-69.

Zaikova, E., D.A. Walsh, C.P. Stillwell, W.W. Mohn, P.D. Tortell, and S.J. Hallam. 2009. Microbial community dynamics in a seasonally anoxic fjord: Saanich Inlet, British Columbia. *Enviro. Microbio*. 12: 172-19.

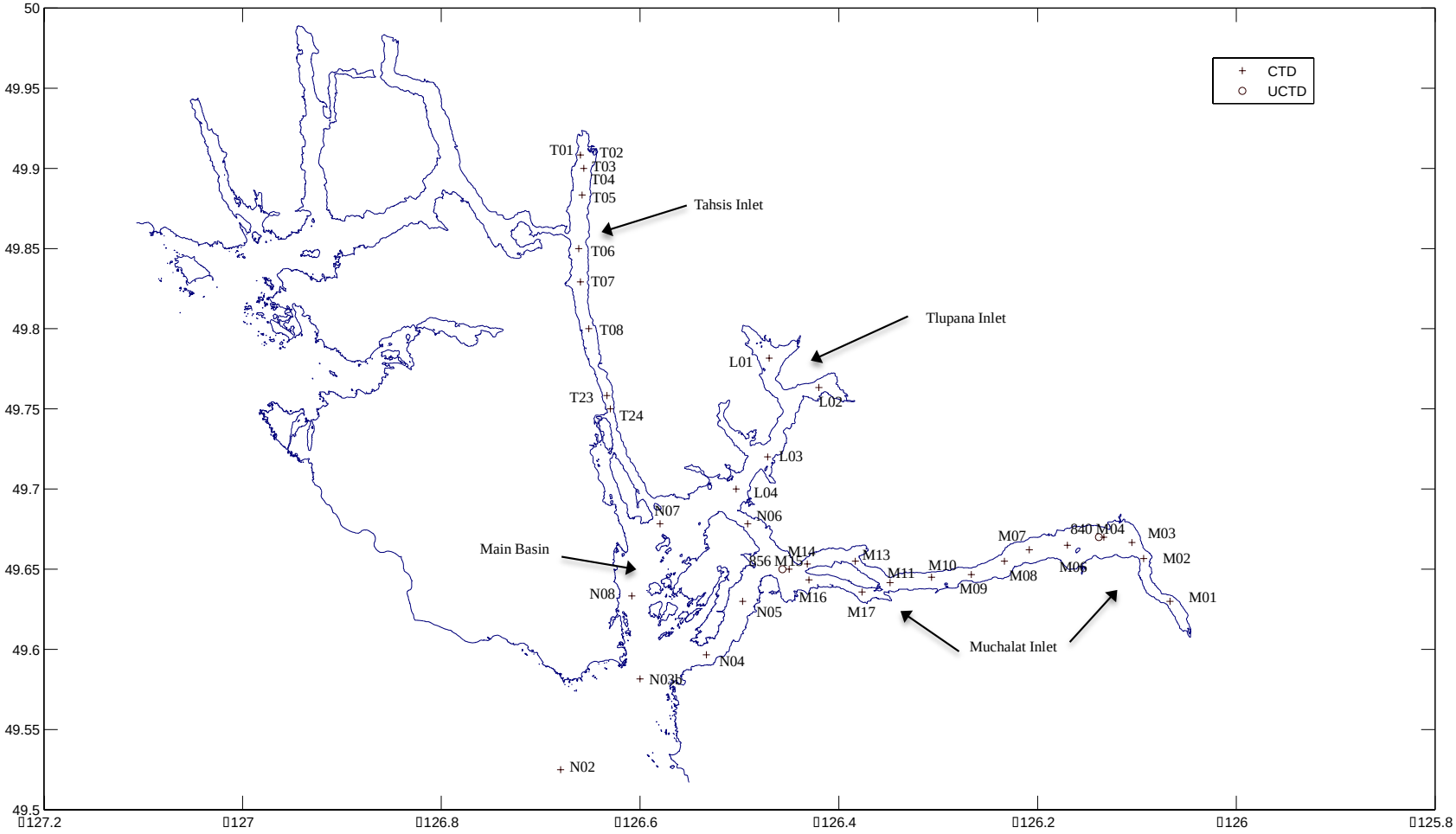

Figure 1. Nootka Sound with labeled inlets and main basin. Marked are CTD stations from all inlets and main basin and UCTD transect beginning (840) and end (856) cast numbers through Muchalat Inlet.

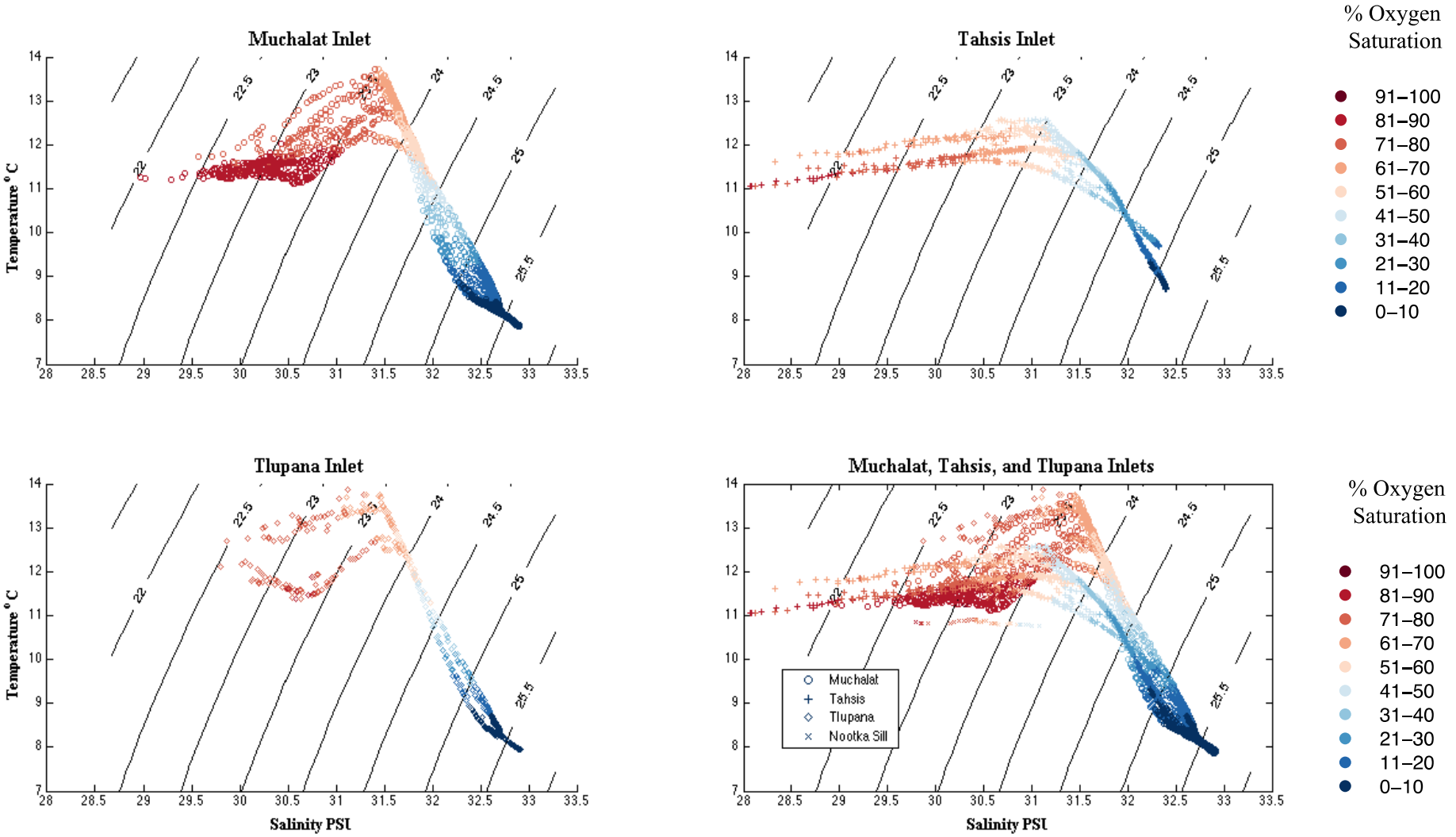

Figure 2. Temperature Salinity plots with lines of constant density. Data points are colored with percent of oxygen saturation. a) Muchalat Inlet. b) Tlupana Inlet. b) Tahsis Inlet. d) All three inlets with the Nootka Sound entrance sill site (Station N02).

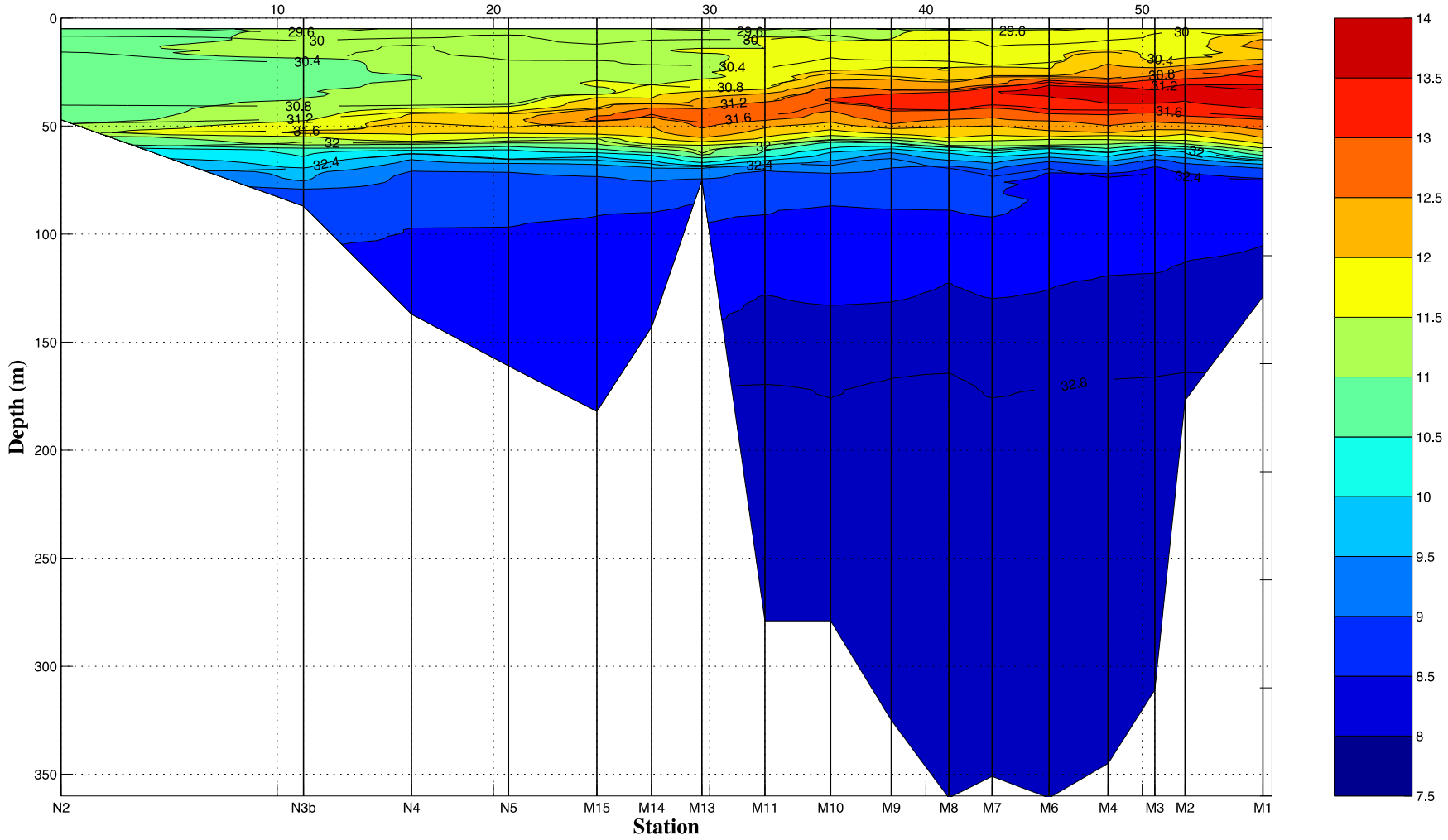

Figure 3. Temperature (color) and salinity (contours) in a section from the Nootka Sound entrance sill through Muchalat Inlet. The horizontal axis gives distance in kilometers from Station N02. Vertical lines mark stationary CTD station locations.

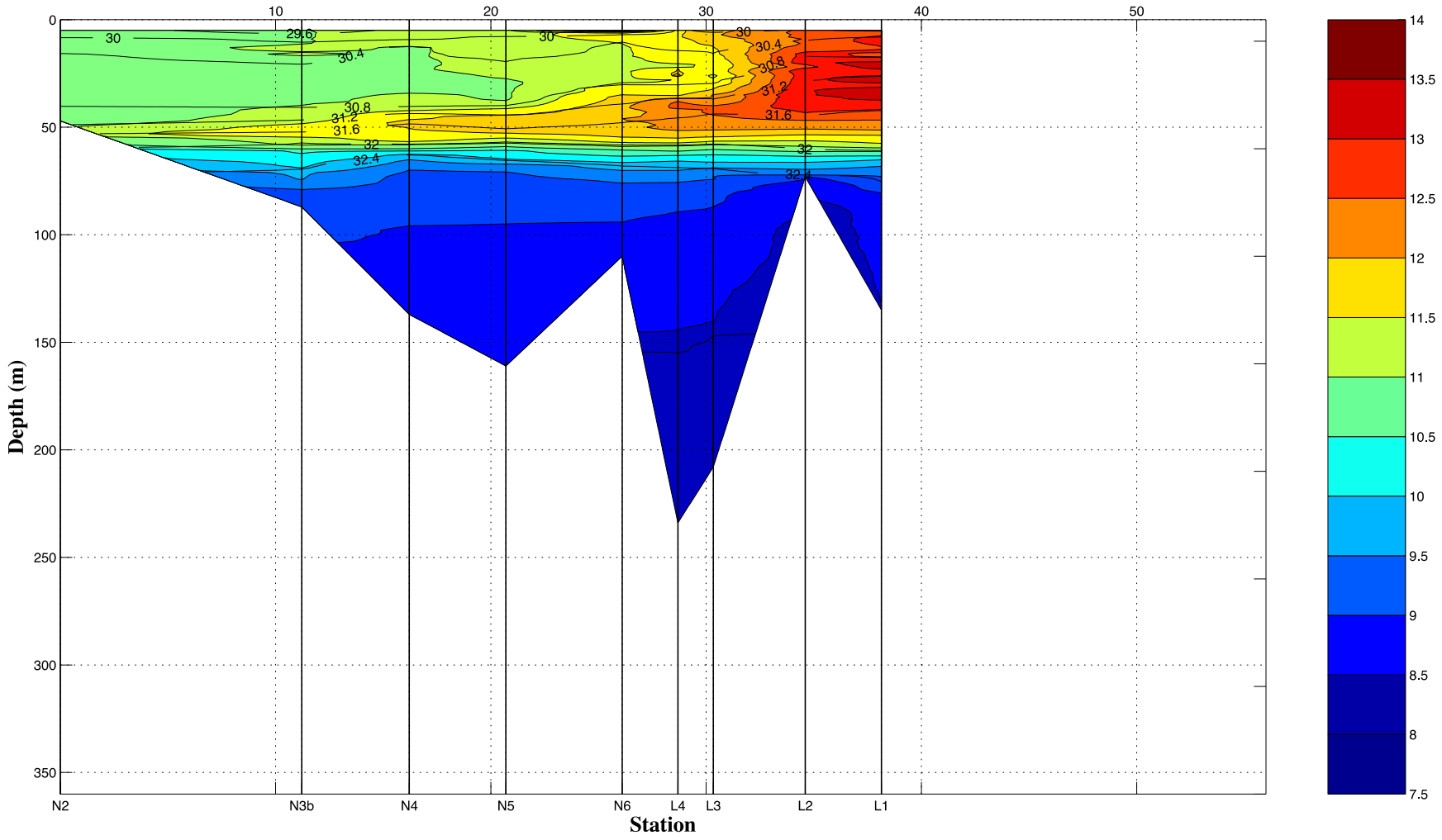

Figure 4. Temperature (color) and salinity (contours) in a section from the Nootka Sound entrance sill through Tlupana Inlet. The horizontal axis gives distance in kilometers from Station N02. Vertical lines mark stationary CTD station locations. The same length and depth scale as Figure 2 is used for comparison.

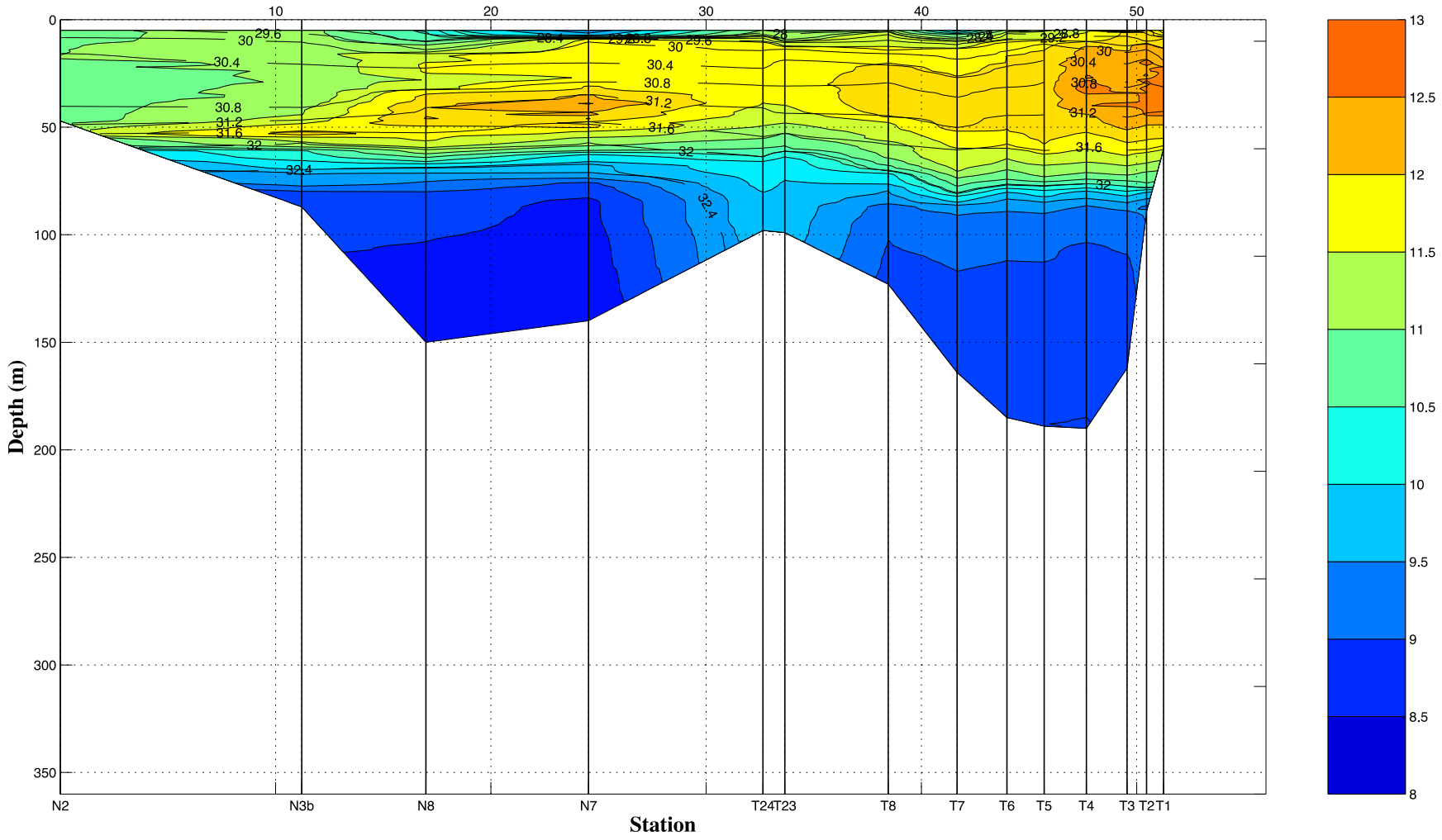

Figure 5. Temperature (color) and salinity (contours) in a section from the Nootka Sound entrance sill through Tahsis Inlet. The horizontal axis gives distance in kilometers from Station N02. Vertical lines mark stationary CTD station locations. The same length and depth scale as Figure 2 is used for comparison.

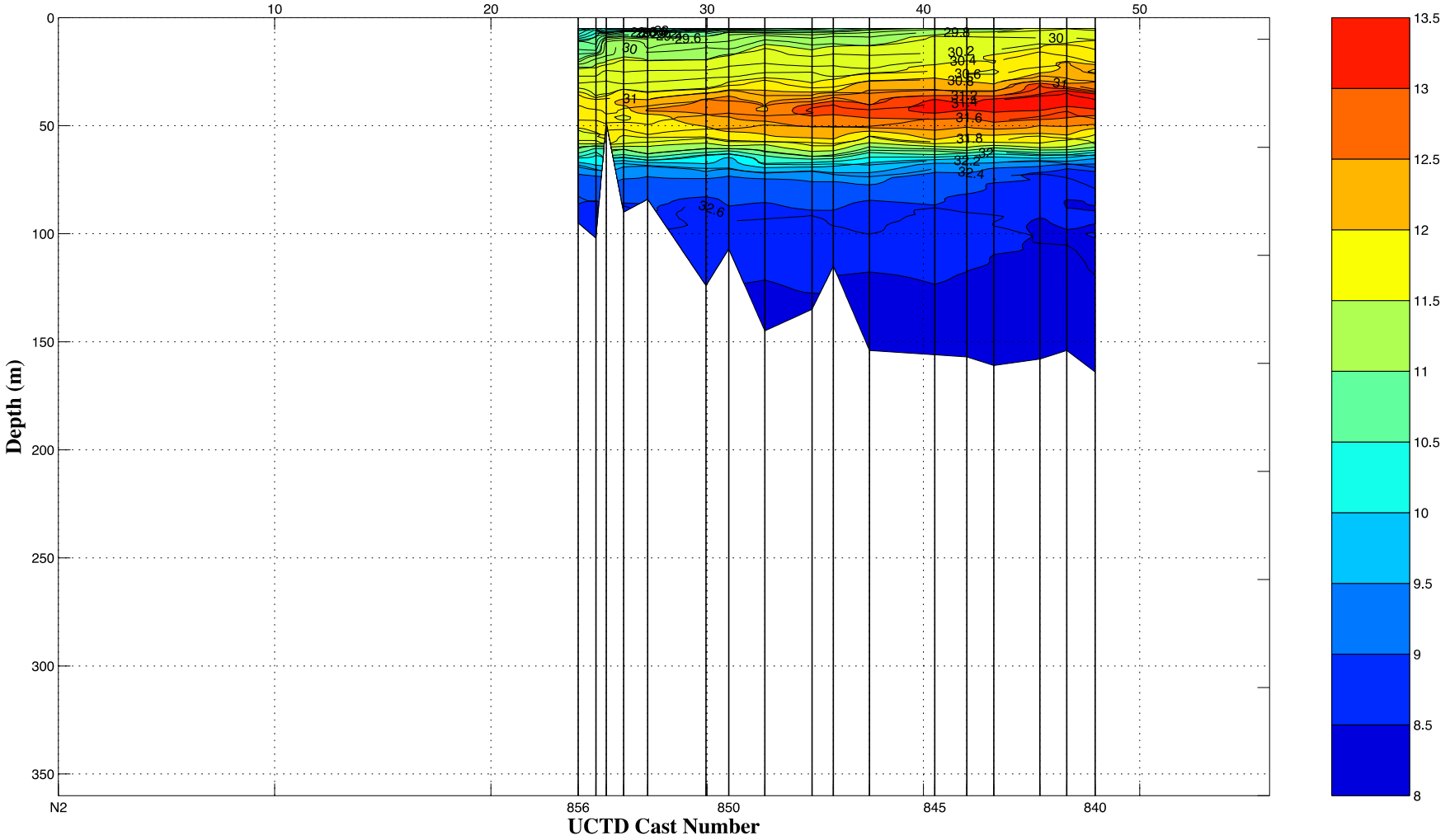

Figure 6. Temperature (color) and salinity (contours) in a section through Muchalat Inlet using UCTD casts. The horizontal axis gives distance in kilometers from Station N02. Vertical lines mark UCTD cast locations. Cast 840 is near CTD station M04 while cast 856 is near CTD station M15. The same length and depth scale as Figure 2 is used for comparison.

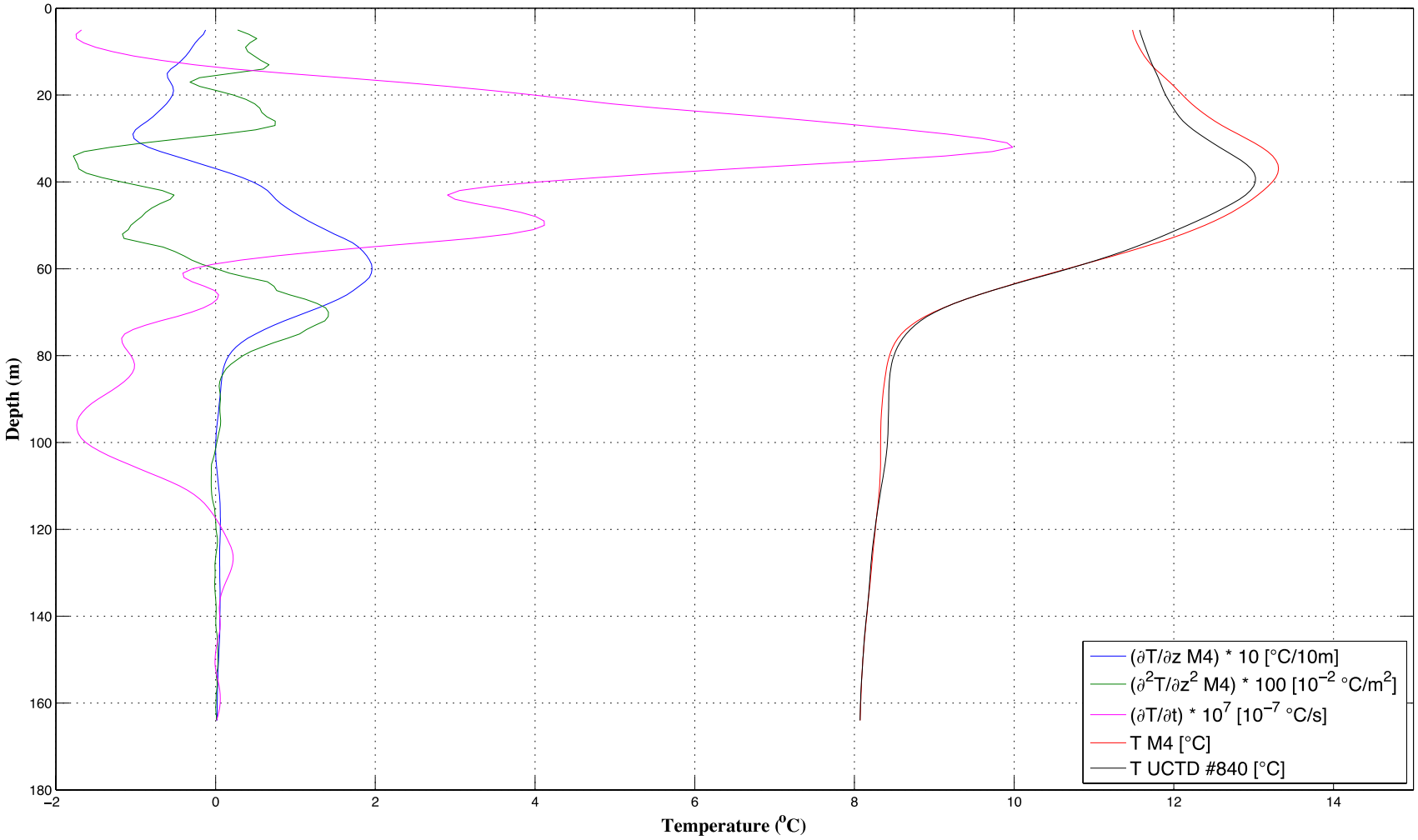

Figure 7. Example plot of CTD and UCTD temperature profile, along with $\frac{\partial T}{\partial z}$ and $\frac{\partial^2 T}{\partial z^2}$ plotted to determine where $\frac{\partial T}{\partial t}$ approaches 0 and $\frac{\partial^2 T}{\partial z^2}$ is robust. Also plotted is an estimate of $\frac{\partial T}{\partial t}$.

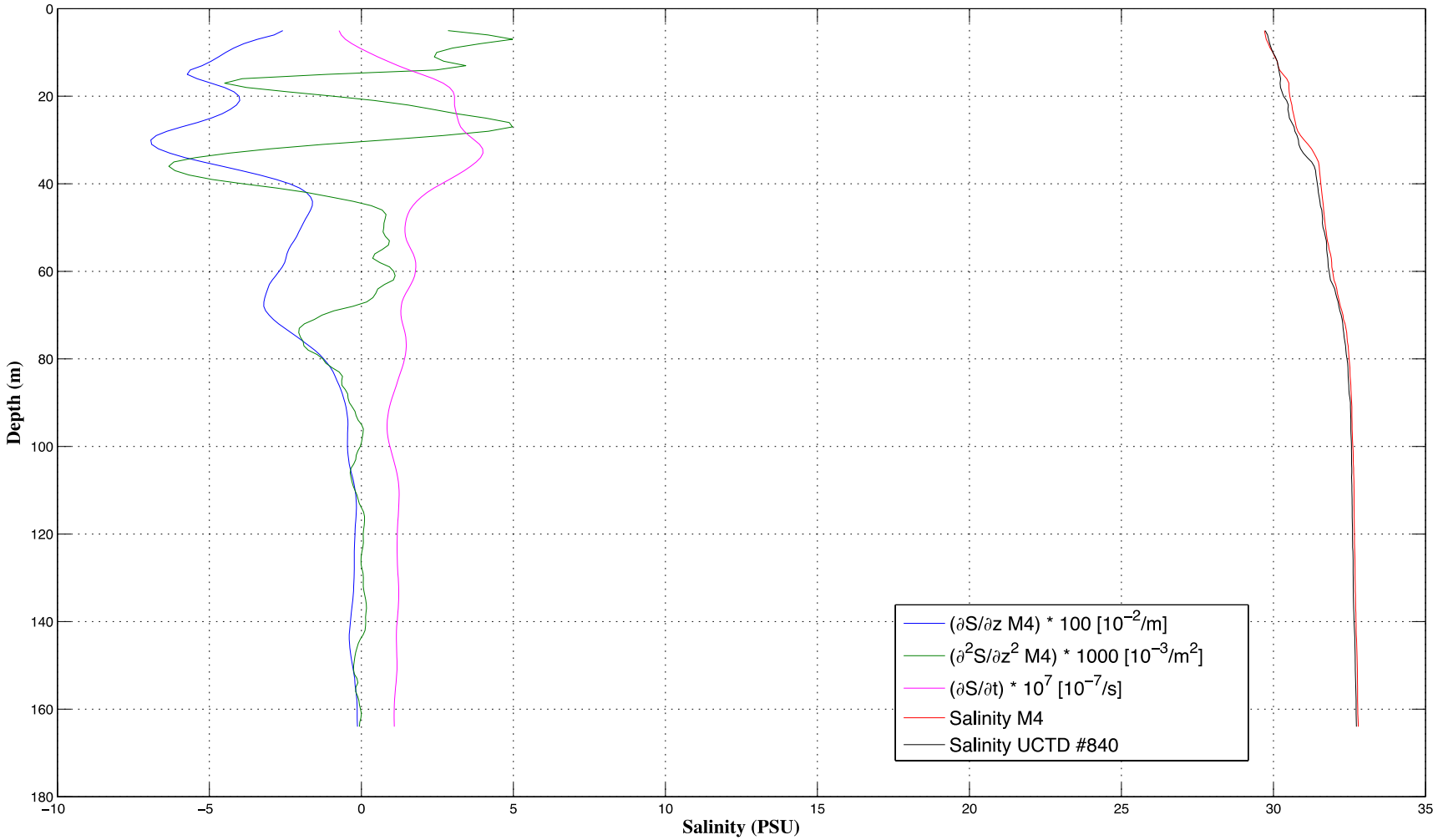

Figure 8. Example plot of CTD and UCTD salinity profile, along with $\frac{\partial S}{\partial z}$ and $\frac{\partial^2 S}{\partial z^2}$ used to determine values consistent with $\frac{\partial T}{\partial t}$ approaching 0 and a robust $\frac{\partial^2 T}{\partial z^2}$. Also plotted is an estimate of $\frac{\partial S}{\partial t}$.